

Investigating the dynamics of a time-dependent barred galaxy model by the Smaller (SALI) and the Generalized (GALI) Alignment Index methods of chaos detection

Haris Skokos

**Department of Mathematics and Applied Mathematics
University of Cape Town, Cape Town, South Africa**

E-mail: haris.skokos@uct.ac.za

URL: http://math_research.uct.ac.za/~hskokos/

**Work in collaboration with
Tassos Bountis, Thanos Manos, Chris Antonopoulos**

Outline

- **Smaller ALignment Index – SALI**
 - ✓ Definition
 - ✓ Behavior for chaotic and regular motion
 - ✓ Applications
- **Generalized ALignment Index – GALI**
 - ✓ Definition - Relation to SALI
 - ✓ Behavior for chaotic and regular motion
 - ✓ Applications
- **Application to a time-dependent barred galaxy model**
- **Summary**

Definition of Smaller Alignment Index (SALI)

Consider the **2N-dimensional** phase space of a conservative dynamical system (**symplectic map or Hamiltonian flow**).

An orbit in that space with initial condition :

$$P(0)=(x_1(0), x_2(0), \dots, x_{2N}(0))$$

and a **deviation vector**

$$v(0)=(\delta x_1(0), \delta x_2(0), \dots, \delta x_{2N}(0))$$

The evolution in time (in maps the time is discrete and is equal to the number n of the iterations) of **a deviation vector** is defined by:

- the **variational equations** (for Hamiltonian flows) and
- the equations of the **tangent map** (for mappings)

Definition of SALI

We follow the evolution in time of two different initial deviation vectors ($\mathbf{v}_1(0)$, $\mathbf{v}_2(0)$), and define SALI (**Ch.S. 2001, J. Phys. A**) as:

$$\text{SALI}(t) = \min \left\{ \left\| \hat{\mathbf{v}}_1(t) + \hat{\mathbf{v}}_2(t) \right\|, \left\| \hat{\mathbf{v}}_1(t) - \hat{\mathbf{v}}_2(t) \right\| \right\}$$

where

$$\hat{\mathbf{v}}_1(t) = \frac{\mathbf{v}_1(t)}{\left\| \mathbf{v}_1(t) \right\|}$$

When the two vectors become **collinear**

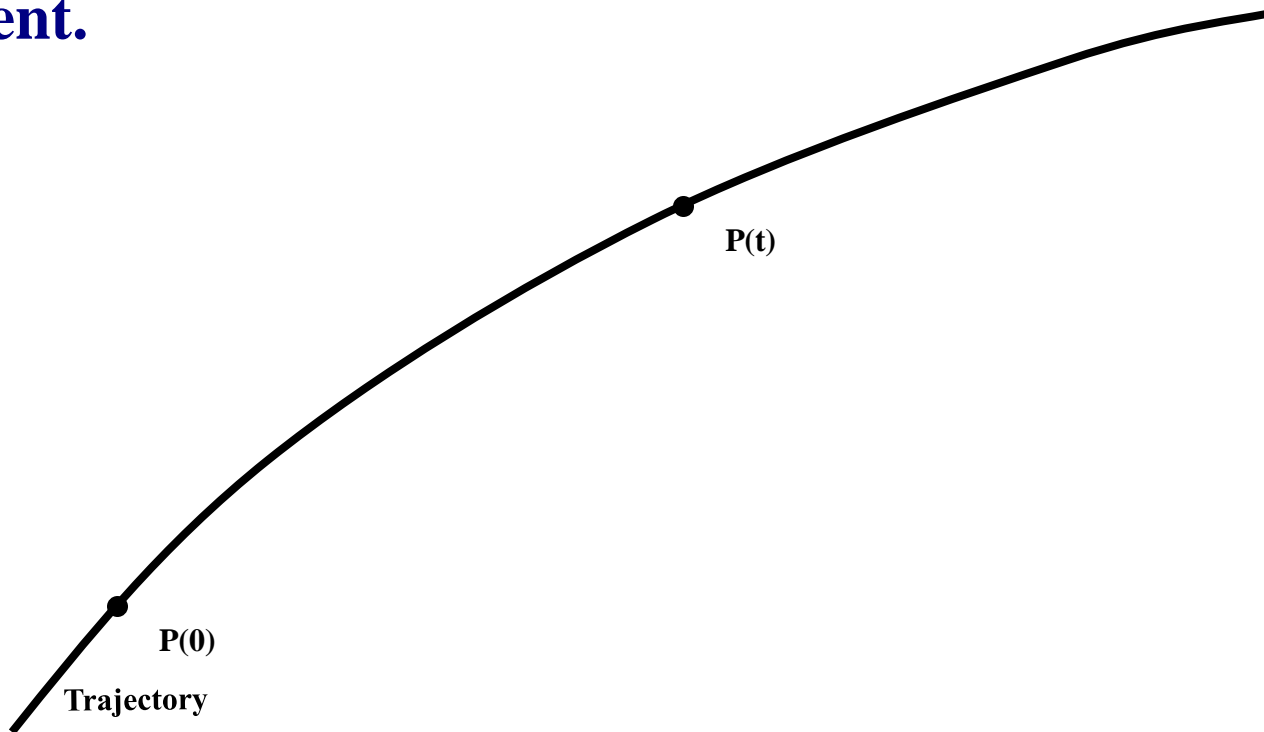
$$\text{SALI}(t) \rightarrow 0$$

Behavior of SALI for chaotic motion

For chaotic orbits the two initially different deviation vectors tend to coincide with the direction defined by the maximum Lyapunov exponent.

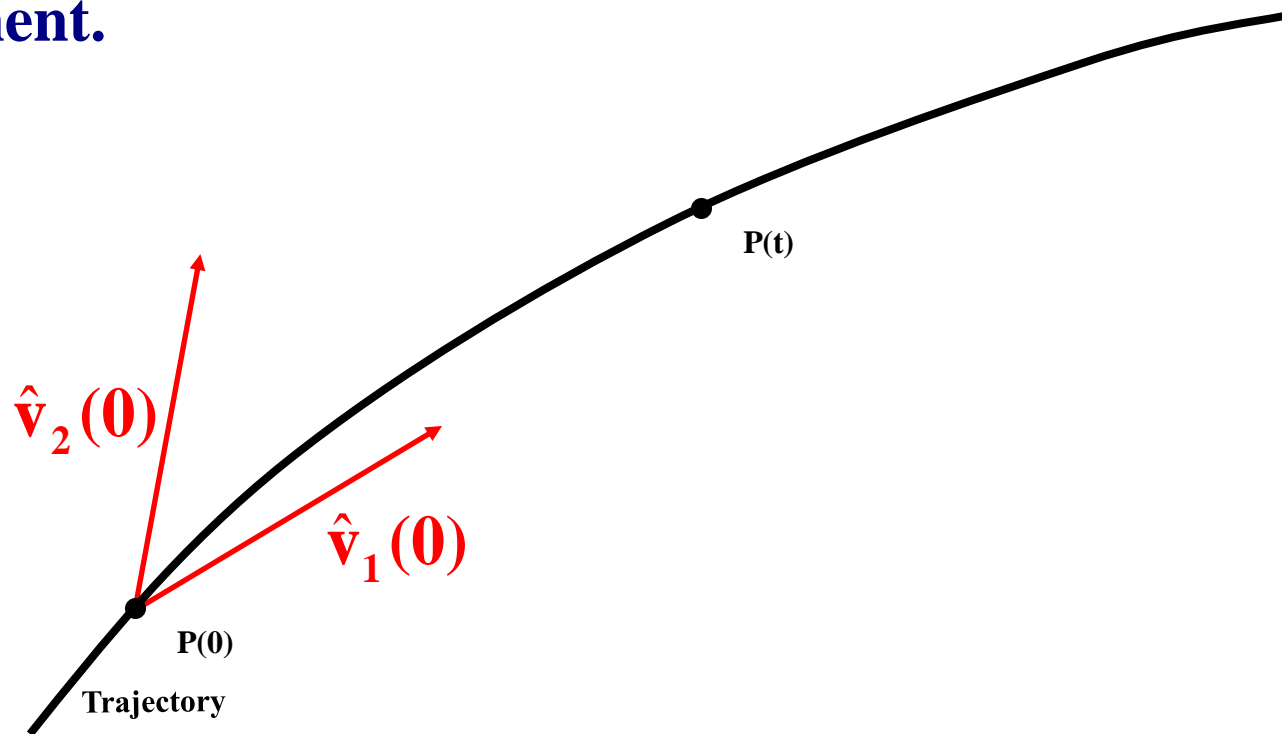
Behavior of SALI for chaotic motion

For chaotic orbits the two initially different deviation vectors tend to coincide with the direction defined by the maximum Lyapunov exponent.



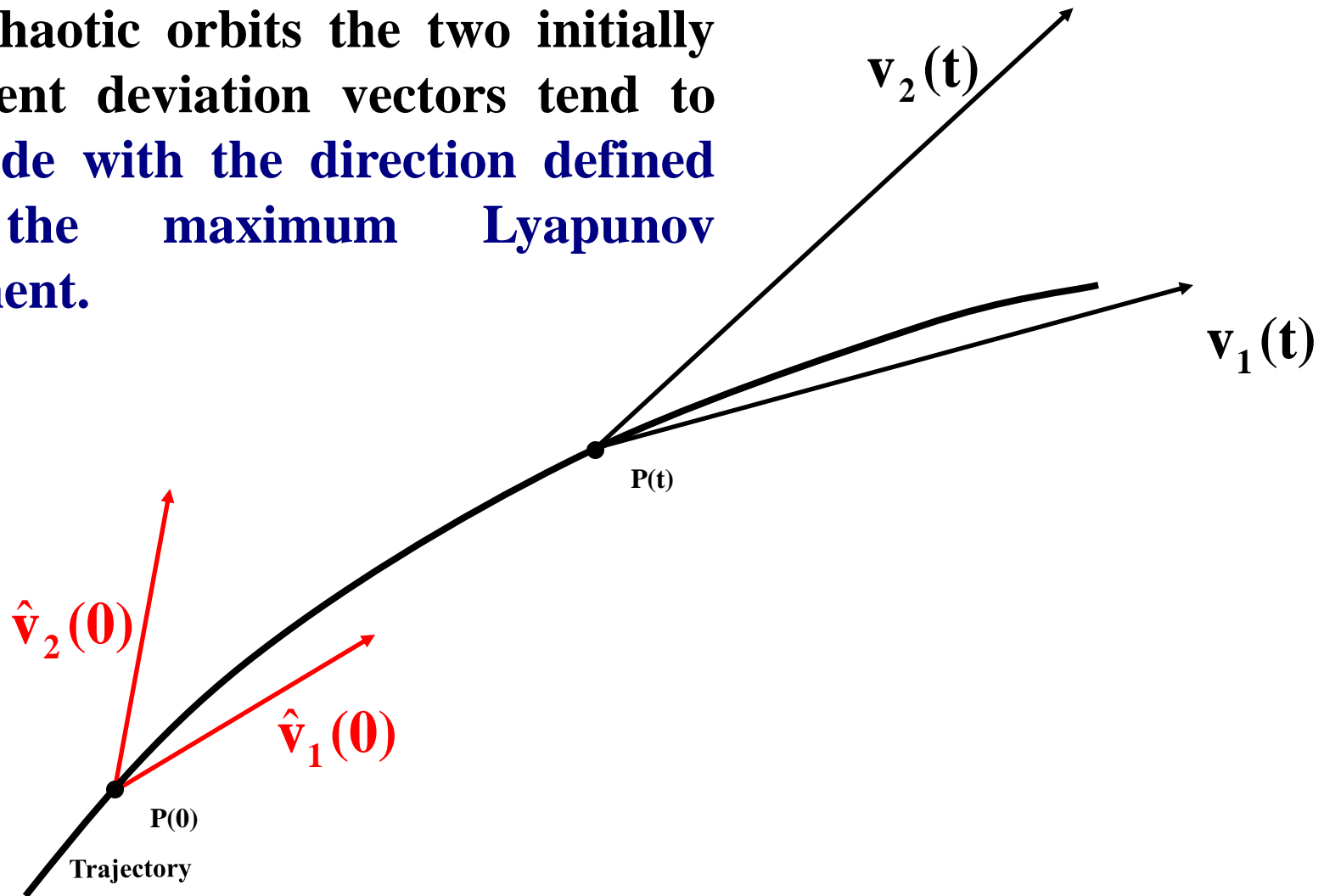
Behavior of SALI for chaotic motion

For chaotic orbits the two initially different deviation vectors tend to coincide with the direction defined by the maximum Lyapunov exponent.



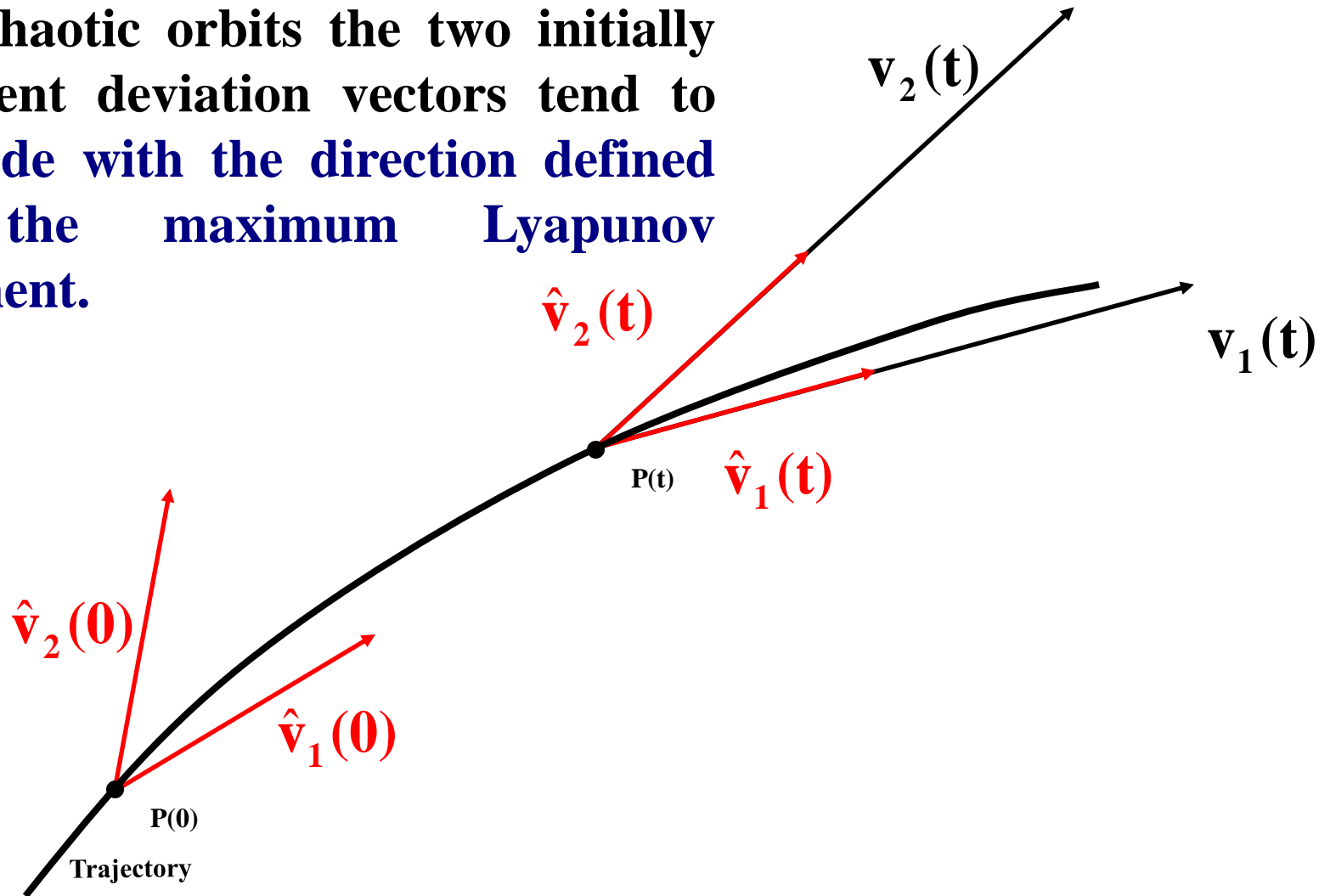
Behavior of SALI for chaotic motion

For chaotic orbits the two initially different deviation vectors tend to coincide with the direction defined by the maximum Lyapunov exponent.



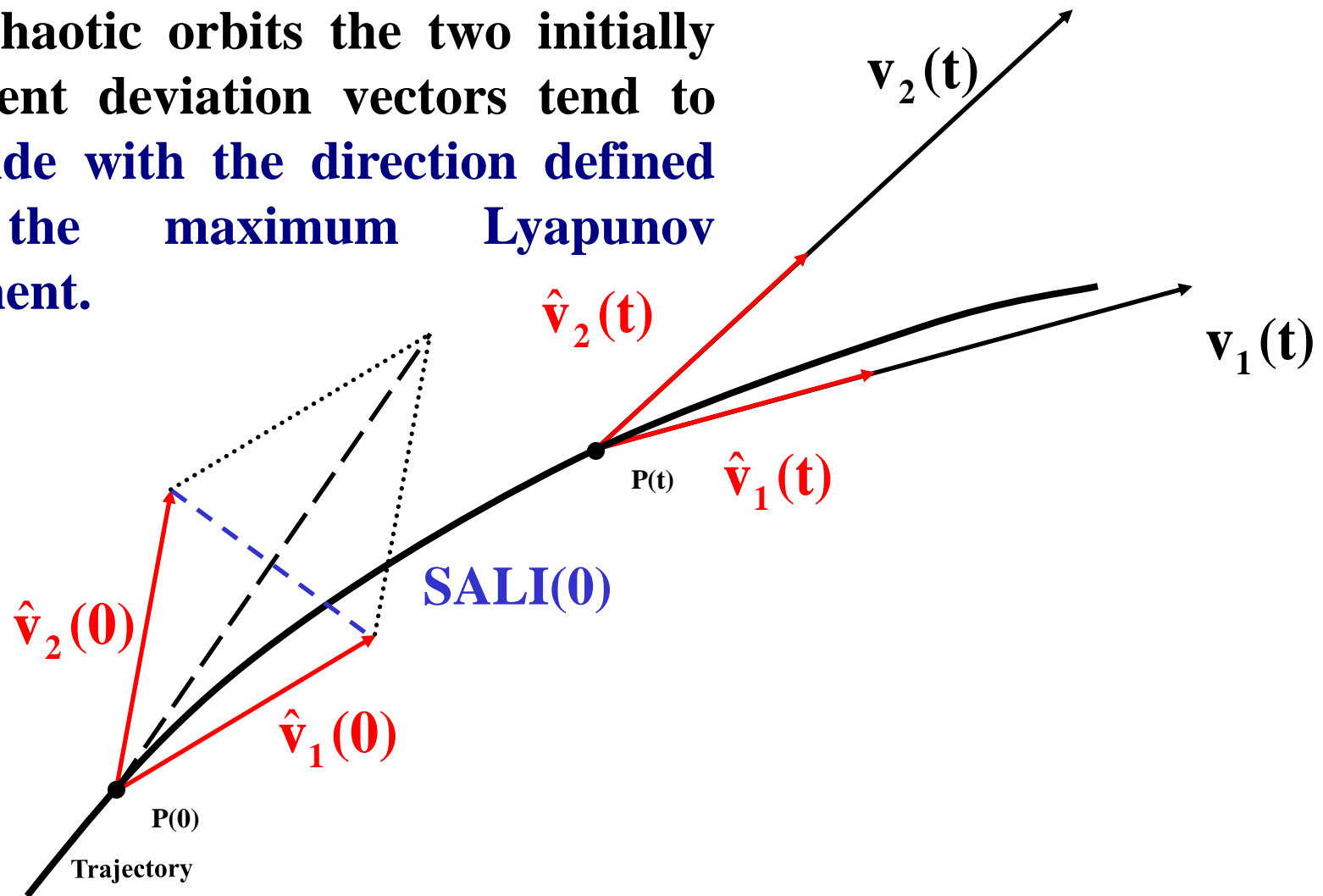
Behavior of SALI for chaotic motion

For chaotic orbits the two initially different deviation vectors tend to coincide with the direction defined by the maximum Lyapunov exponent.



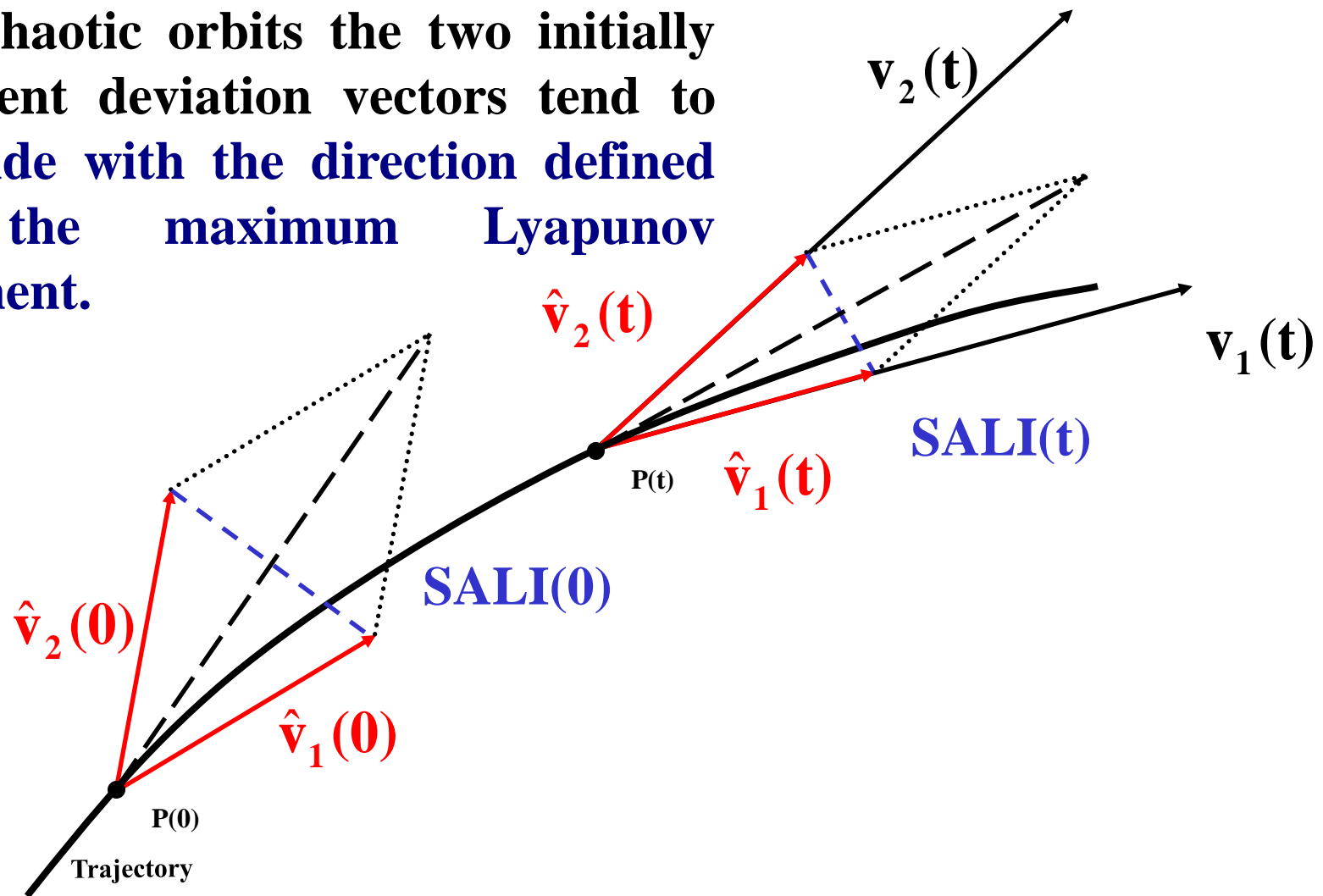
Behavior of SALI for chaotic motion

For chaotic orbits the two initially different deviation vectors tend to coincide with the direction defined by the maximum Lyapunov exponent.



Behavior of SALI for chaotic motion

For chaotic orbits the two initially different deviation vectors tend to coincide with the direction defined by the maximum Lyapunov exponent.

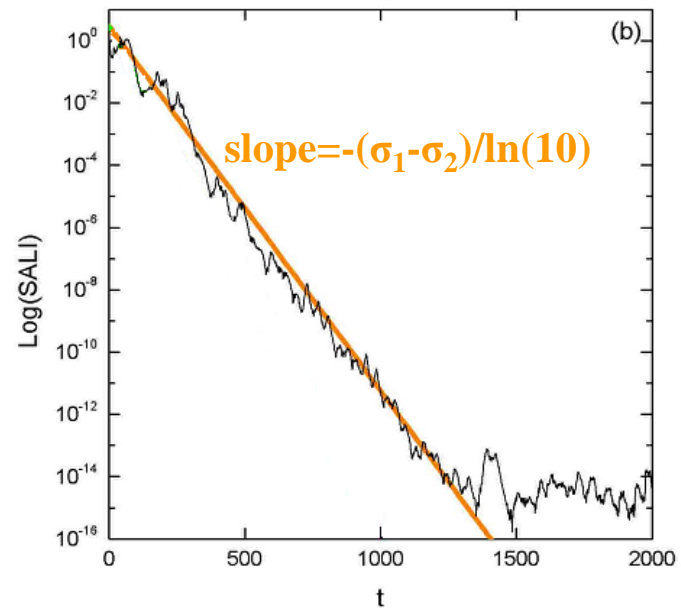
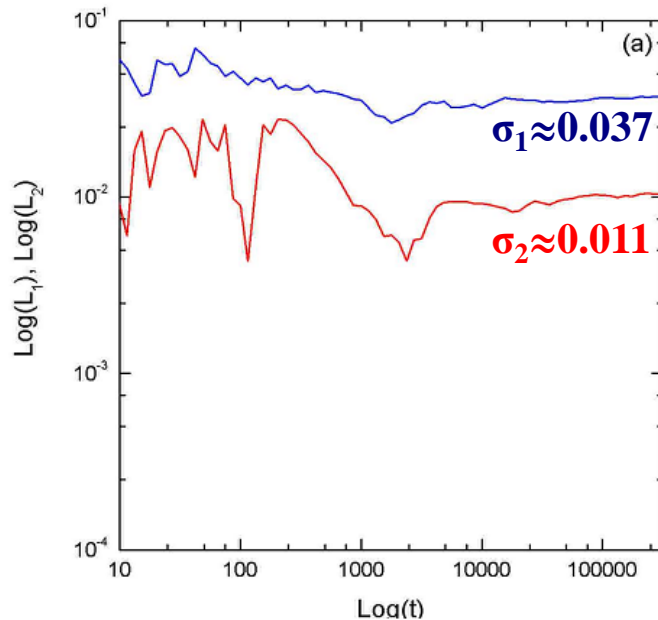


Behavior of SALI for chaotic motion

We test the validity of the approximation $\text{SALI} \propto e^{-(\sigma_1 - \sigma_2)t}$ (Ch.S., Antonopoulos, Bountis, Vrahatis, 2004, J. Phys. A) for a chaotic orbit of the 3D Hamiltonian

$$H = \sum_{i=1}^3 \frac{\omega_i}{2} (q_i^2 + p_i^2) + q_1^2 q_2 + q_1^2 q_3$$

with $\omega_1=1$, $\omega_2=1.4142$, $\omega_3=1.7321$, $H=0.09$

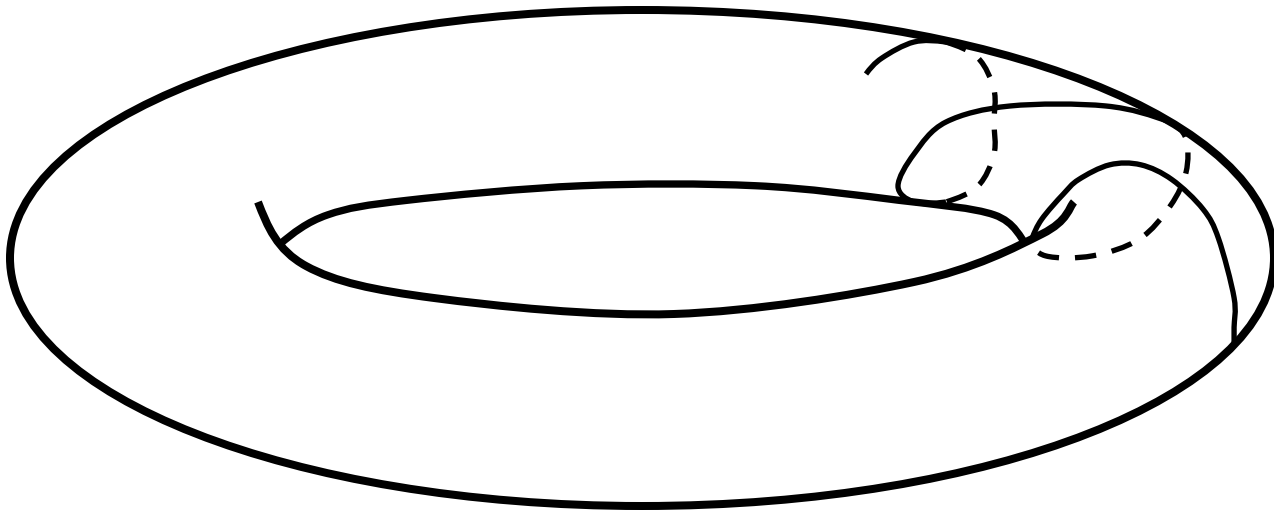


Behavior of SALI for regular motion

Regular motion occurs on a torus and two different initial deviation vectors become tangent to the torus, generally having different directions.

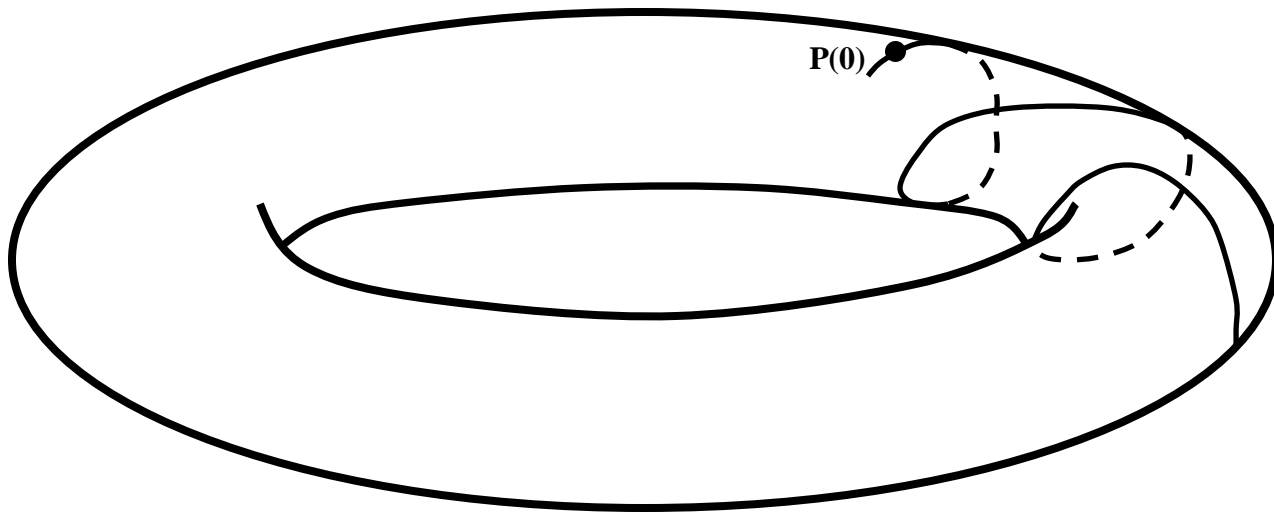
Behavior of SALI for **regular motion**

Regular motion occurs on a torus and two different initial deviation vectors **become tangent to the torus, generally having different directions.**



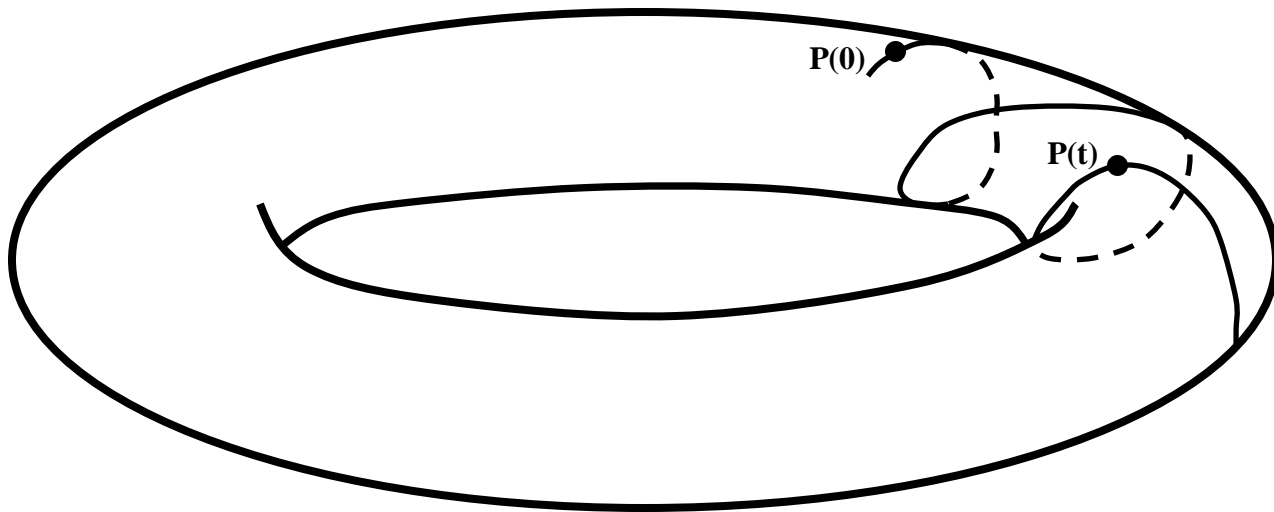
Behavior of SALI for **regular motion**

Regular motion occurs on a torus and two different initial deviation vectors **become tangent to the torus, generally having different directions.**



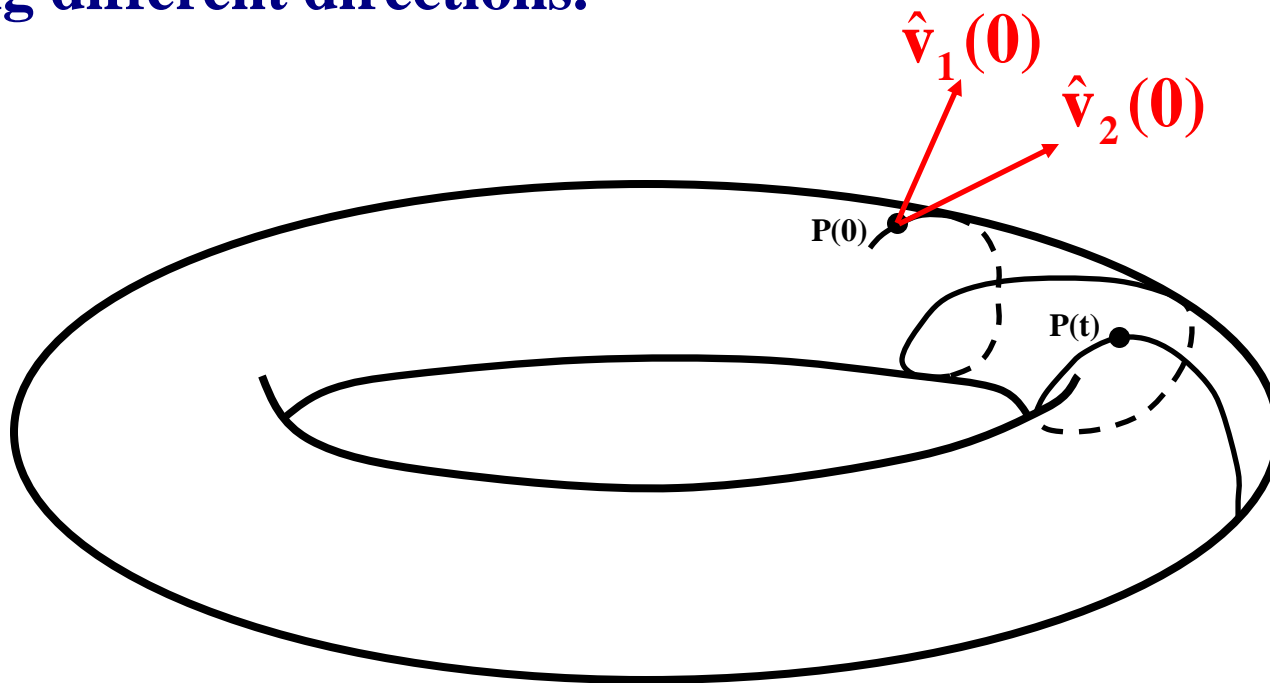
Behavior of SALI for **regular motion**

Regular motion occurs on a torus and two different initial deviation vectors **become tangent to the torus, generally having different directions.**



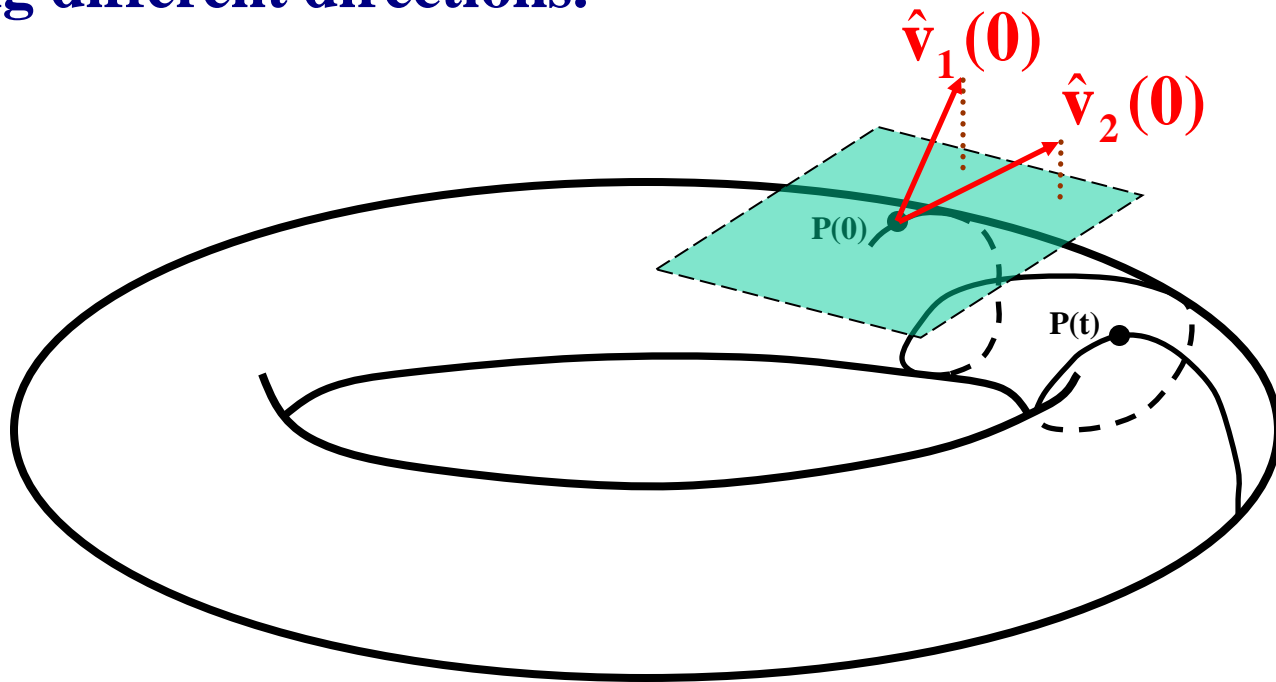
Behavior of SALI for **regular motion**

Regular motion occurs on a torus and two different initial deviation vectors **become tangent to the torus**, generally **having different directions**.



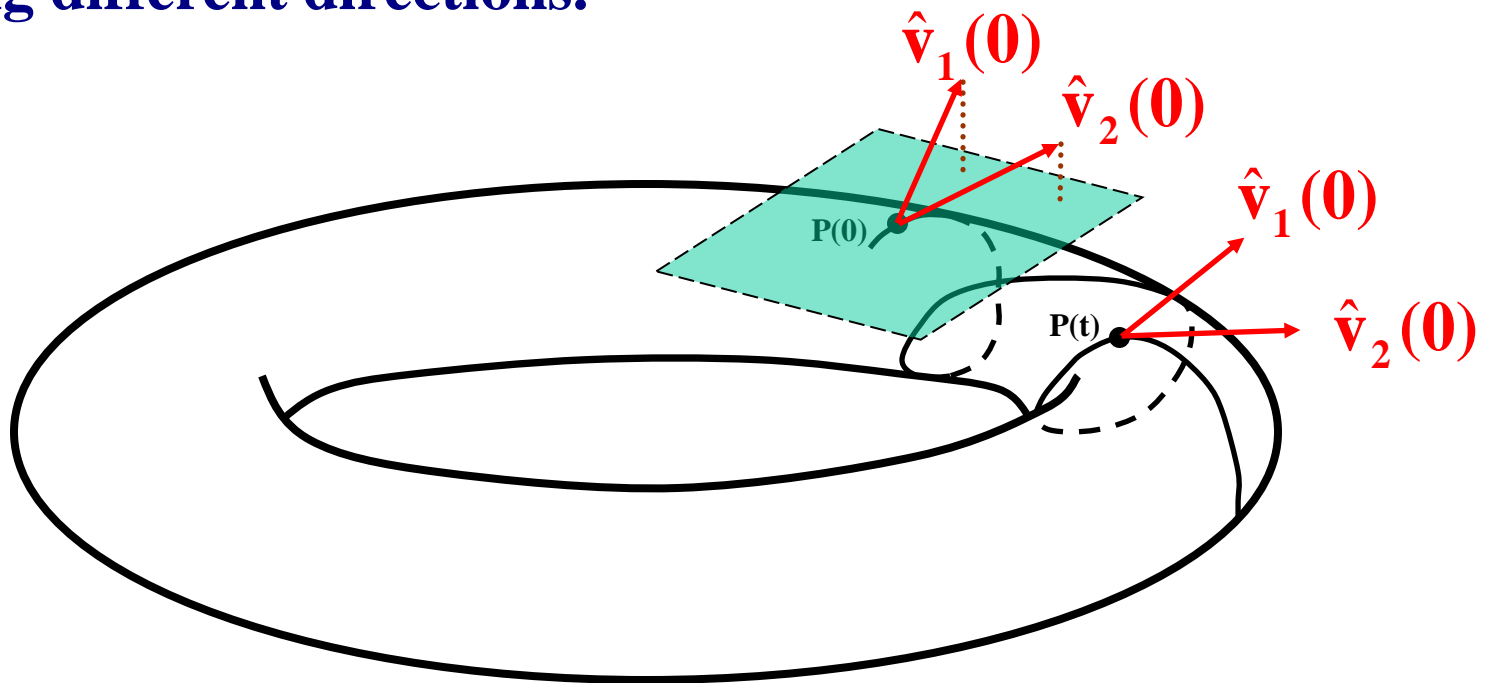
Behavior of SALI for **regular motion**

Regular motion occurs on a torus and two different initial deviation vectors **become tangent to the torus**, generally **having different directions**.



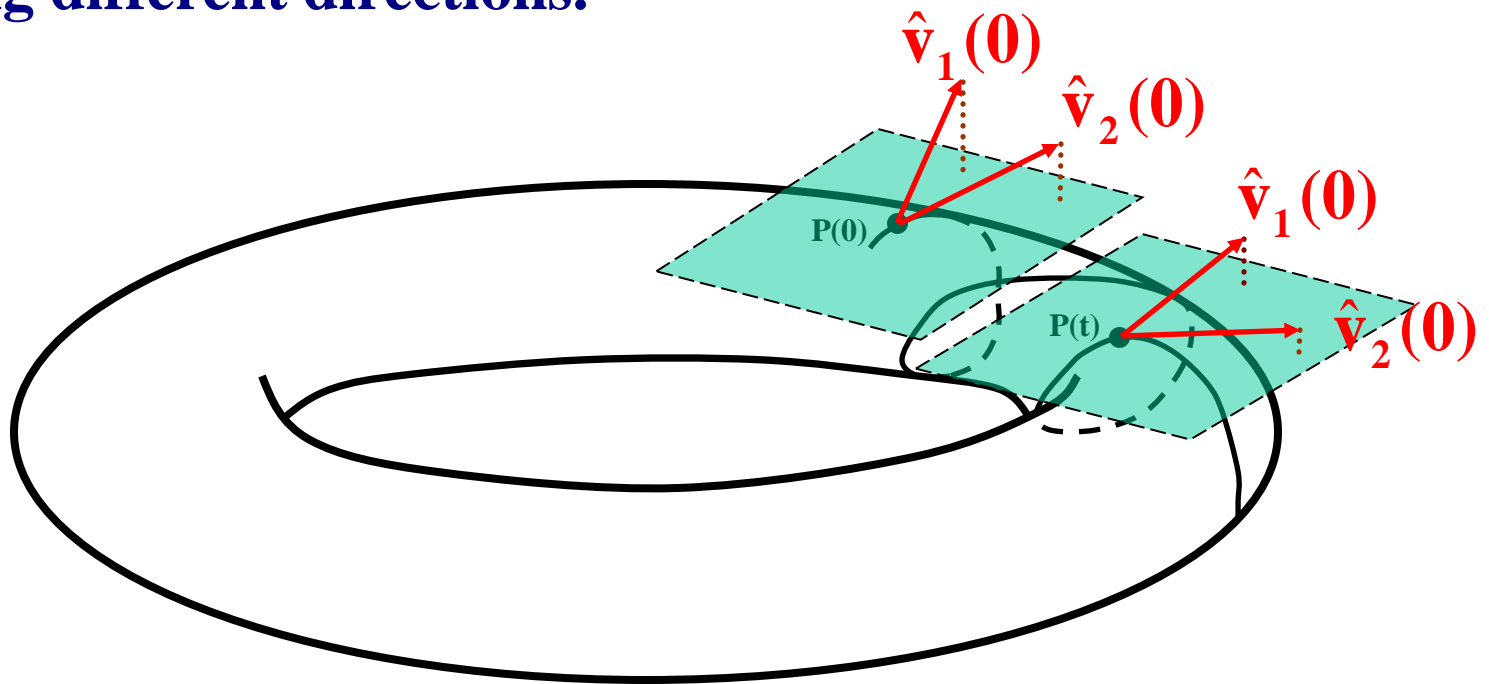
Behavior of SALI for **regular motion**

Regular motion occurs on a torus and two different initial deviation vectors **become tangent to the torus**, generally having different directions.



Behavior of SALI for **regular motion**

Regular motion occurs on a torus and two different initial deviation vectors **become tangent to the torus**, generally having different directions.



Applications – Hénon-Heiles system

As an example, we consider the 2D Hénon-Heiles system:

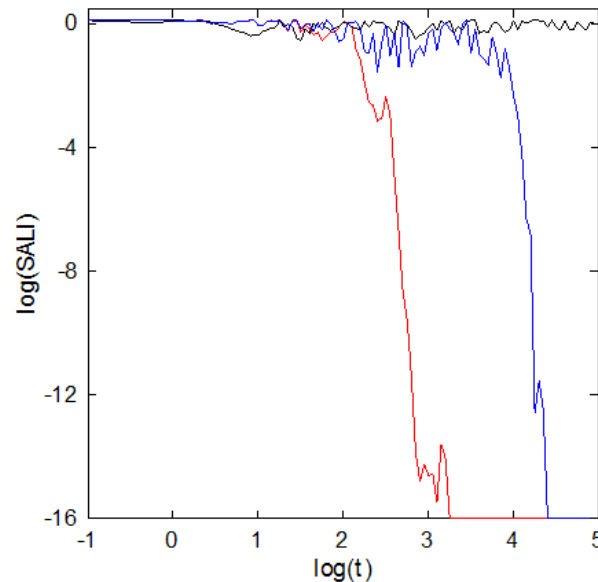
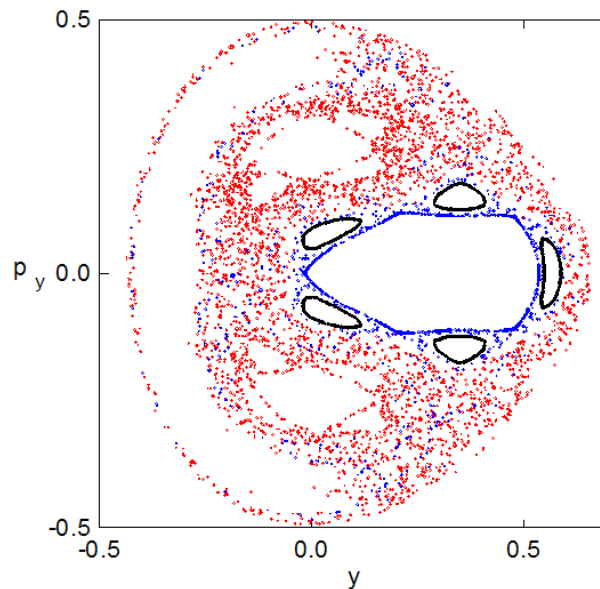
$$H_2 = \frac{1}{2}(p_x^2 + p_y^2) + \frac{1}{2}(x^2 + y^2) + x^2y - \frac{1}{3}y^3$$

For $E=1/8$ we consider the orbits with initial conditions:

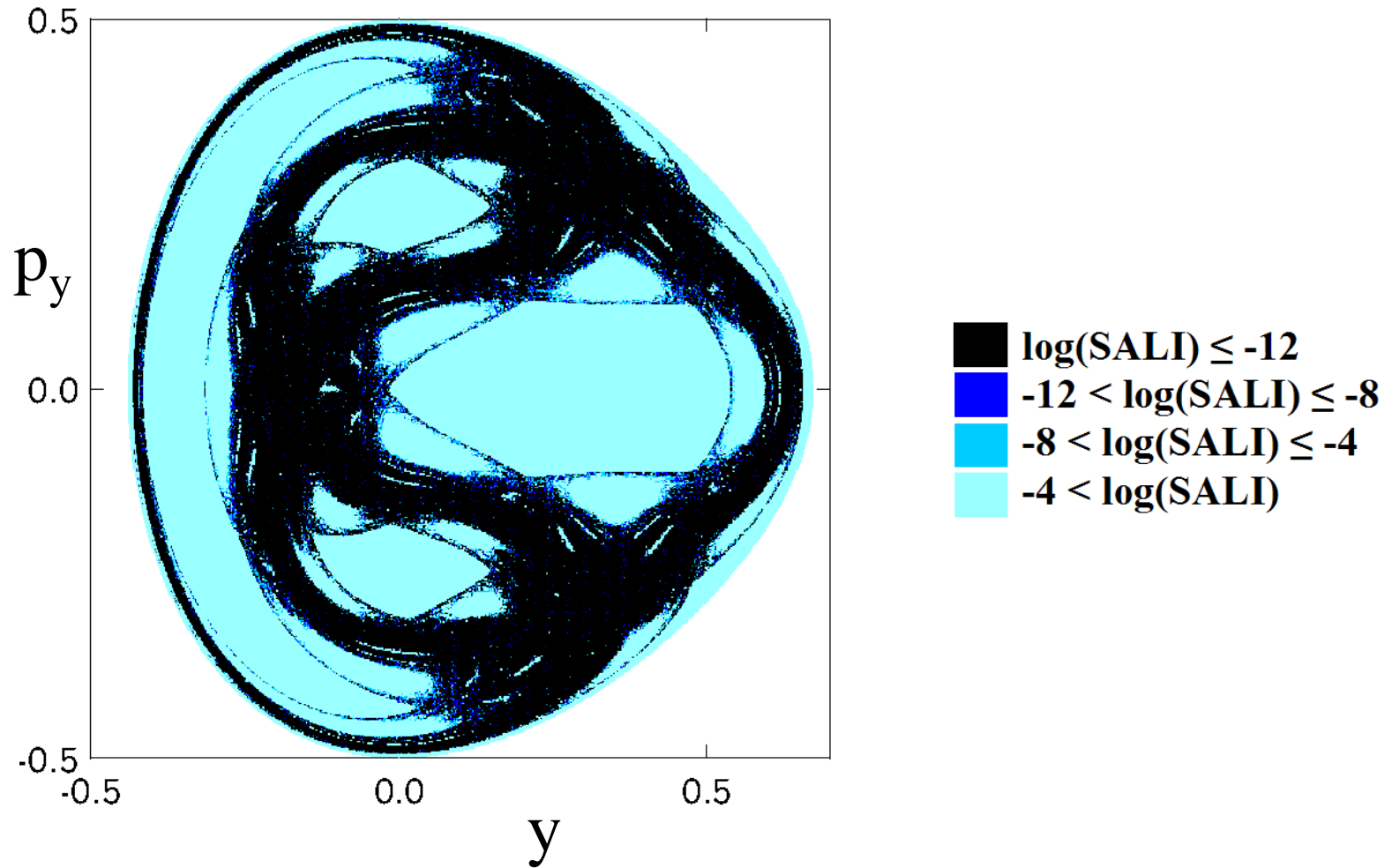
Regular orbit, $x=0$, $y=0.55$, $p_x=0.2417$, $p_y=0$

Chaotic orbit, $x=0$, $y=-0.016$, $p_x=0.49974$, $p_y=0$

Chaotic orbit, $x=0$, $y=-0.01344$, $p_x=0.49982$, $p_y=0$



Applications – Hénon-Heiles system



Questions

Can we generalize SALI so that the new index:

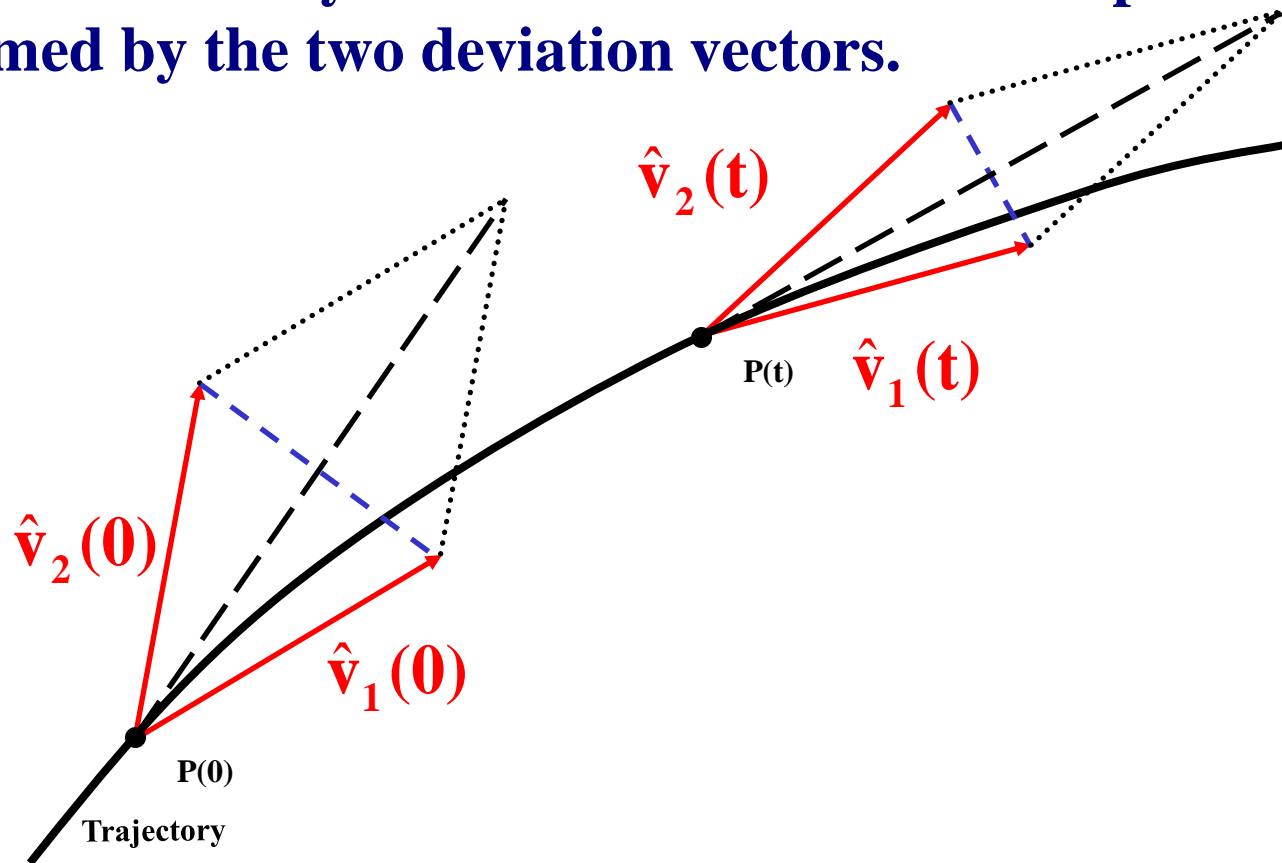
- **Can rapidly reveal the nature of chaotic orbits with $\sigma_1 \approx \sigma_2$ ($\text{SALI} \propto e^{-(\sigma_1 - \sigma_2)t}$)?**
- **Depends on several Lyapunov exponents for chaotic orbits?**

Definition of Generalized Alignment Index (GALI)

SALI effectively measures the 'area' of the parallelogram formed by the two deviation vectors.

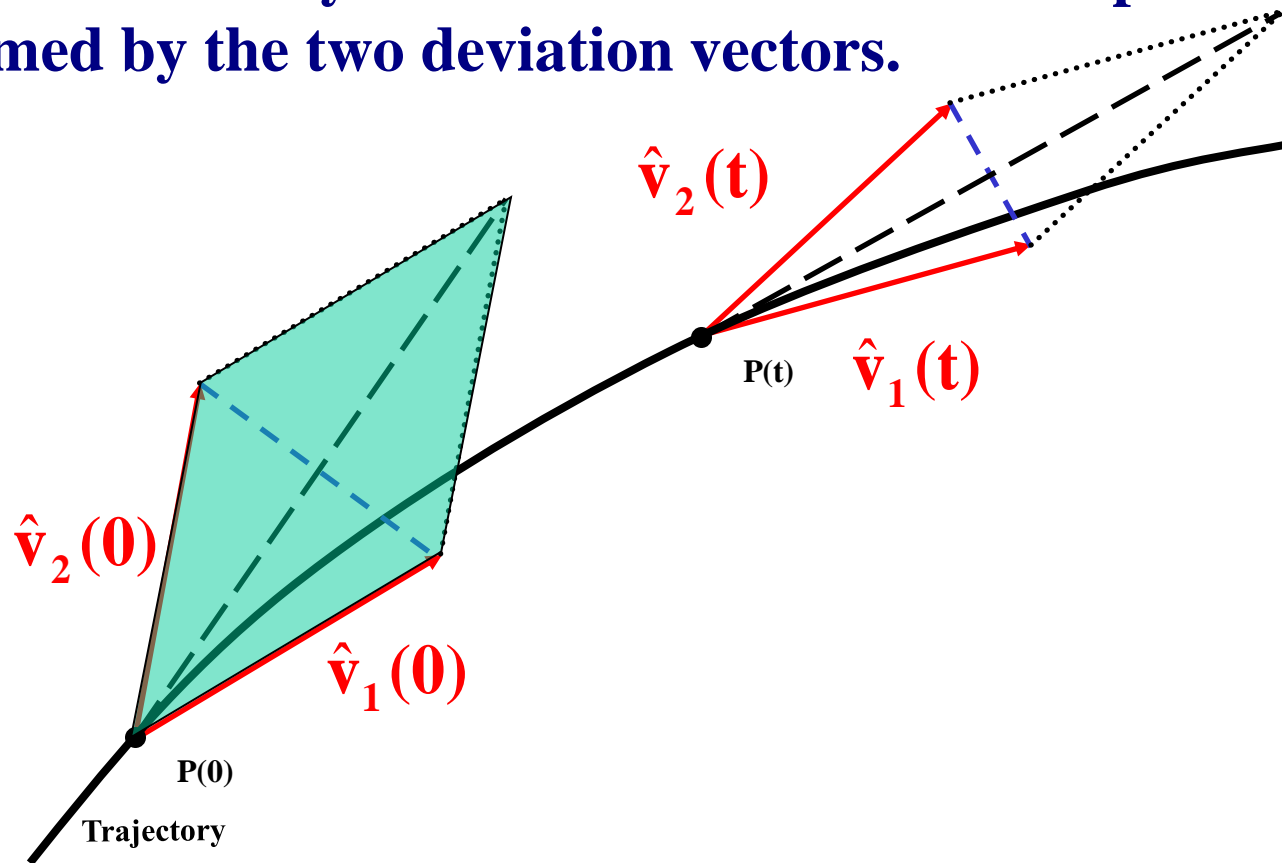
Definition of Generalized Alignment Index (GALI)

SALI effectively measures the 'area' of the parallelogram formed by the two deviation vectors.



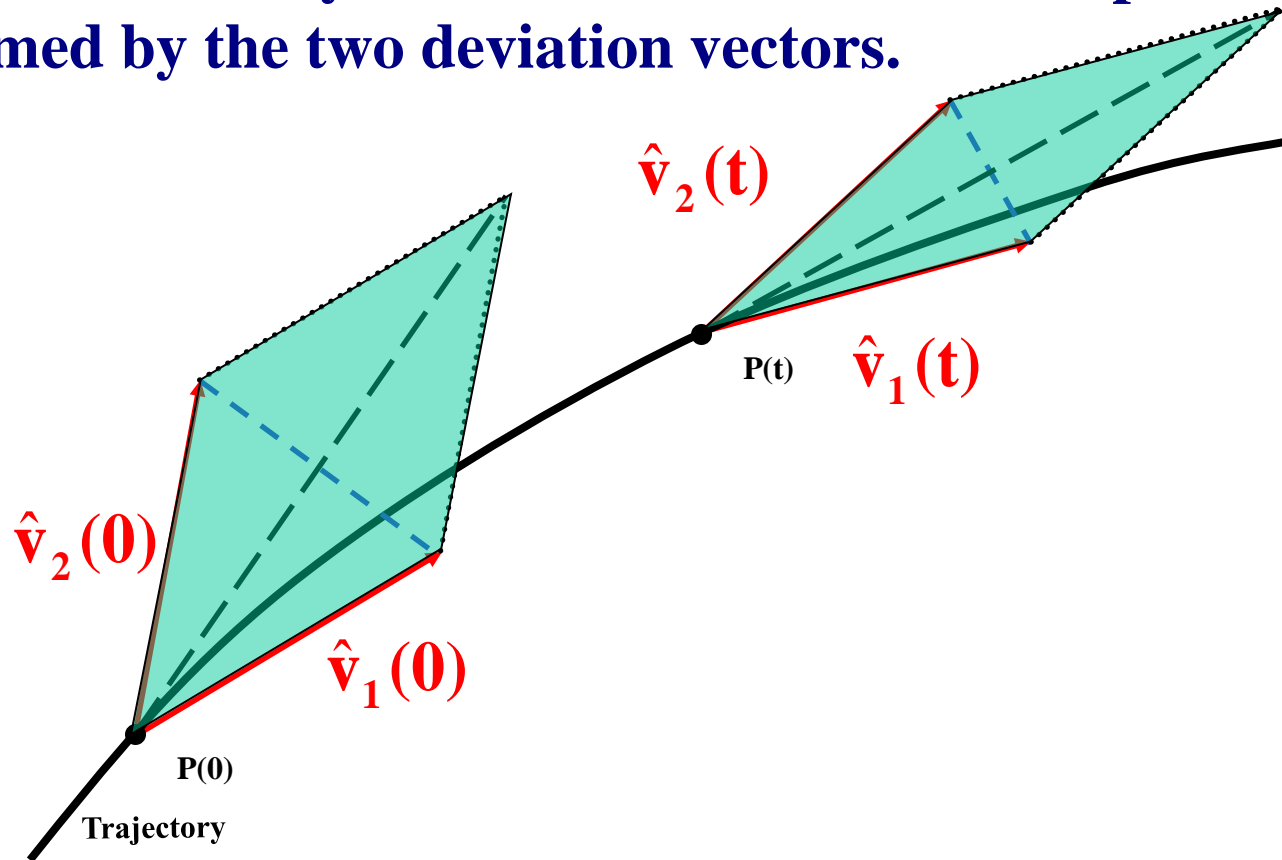
Definition of Generalized Alignment Index (GALI)

SALI effectively measures the 'area' of the parallelogram formed by the two deviation vectors.



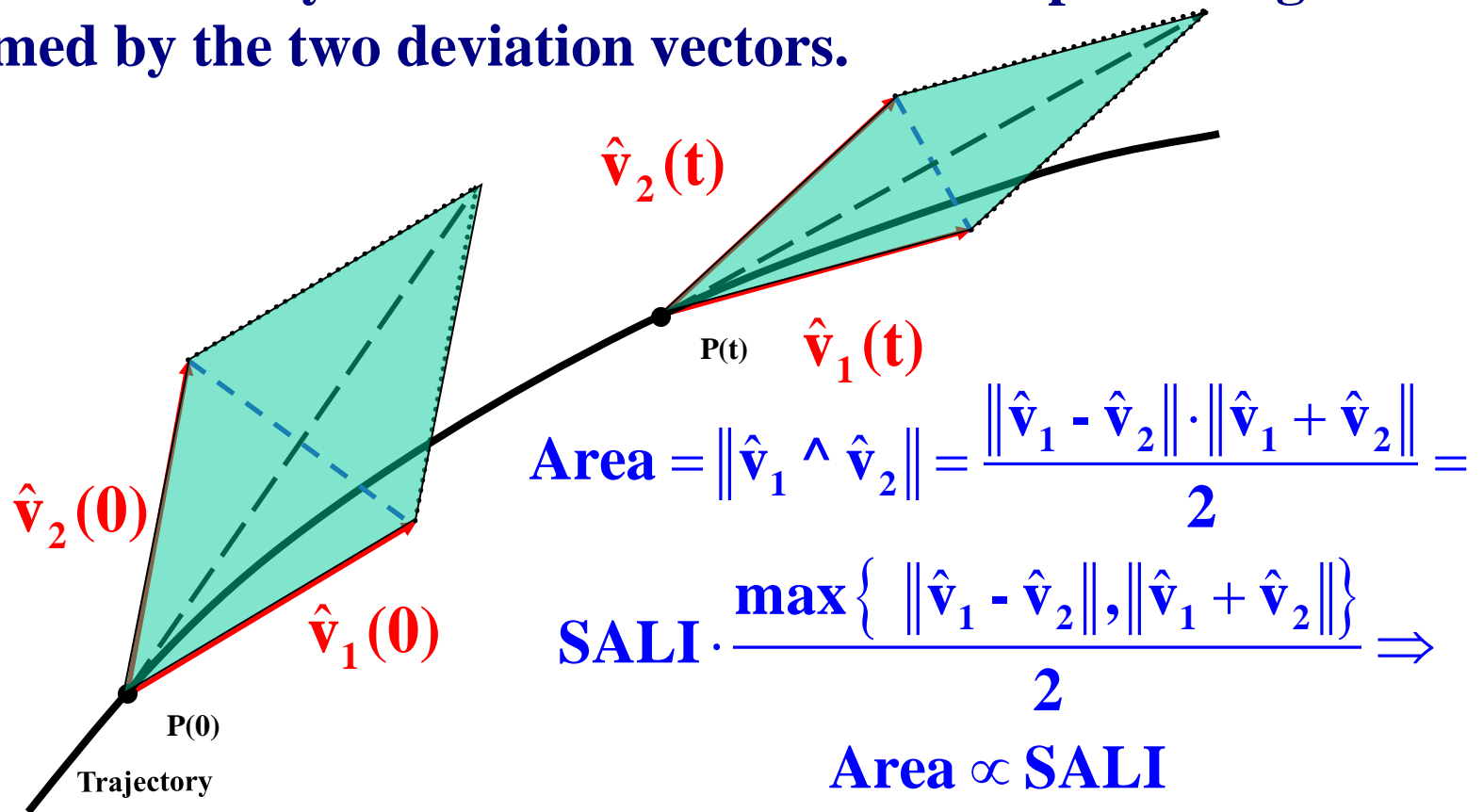
Definition of Generalized Alignment Index (GALI)

SALI effectively measures the 'area' of the parallelogram formed by the two deviation vectors.



Definition of Generalized Alignment Index (GALI)

SALI effectively measures the ‘area’ of the parallelogram formed by the two deviation vectors.



Definition of GALI

In the case of an N degree of freedom Hamiltonian system or a $2N$ symplectic map we follow the evolution of

k deviation vectors with $2 \leq k \leq 2N$,

and define (Ch.S., Bountis, Antonopoulos, 2007, Physica D) the Generalized Alignment Index (GALI) of order k :

$$\text{GALI}_k(t) = \|\hat{\mathbf{v}}_1(t) \wedge \hat{\mathbf{v}}_2(t) \wedge \dots \wedge \hat{\mathbf{v}}_k(t)\|$$

where

$$\hat{\mathbf{v}}_1(t) = \frac{\mathbf{v}_1(t)}{\|\mathbf{v}_1(t)\|}$$

Behavior of $GALI_k$ for chaotic motion

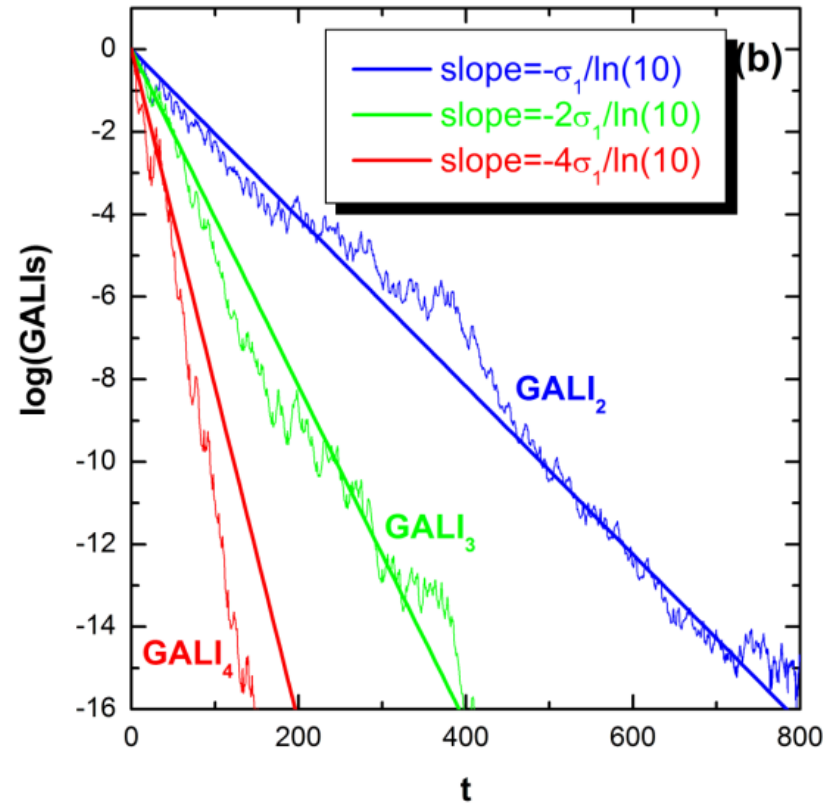
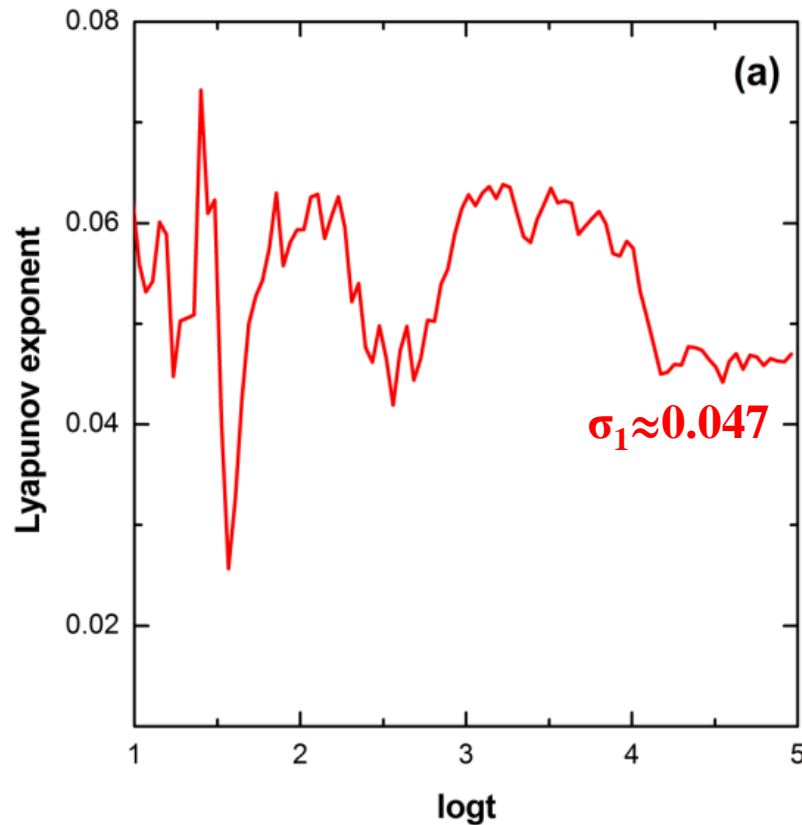
$GALI_k$ ($2 \leq k \leq 2N$) tends exponentially to zero with exponents that involve the values of the first k largest Lyapunov exponents $\sigma_1, \sigma_2, \dots, \sigma_k$:

$$GALI_k(t) \propto e^{-[(\sigma_1 - \sigma_2) + (\sigma_1 - \sigma_3) + \dots + (\sigma_1 - \sigma_k)]t}$$

The above relation is valid even if some Lyapunov exponents are equal, or very close to each other.

Behavior of GALI_k for chaotic motion

2D Hamiltonian (Hénon-Heiles system)

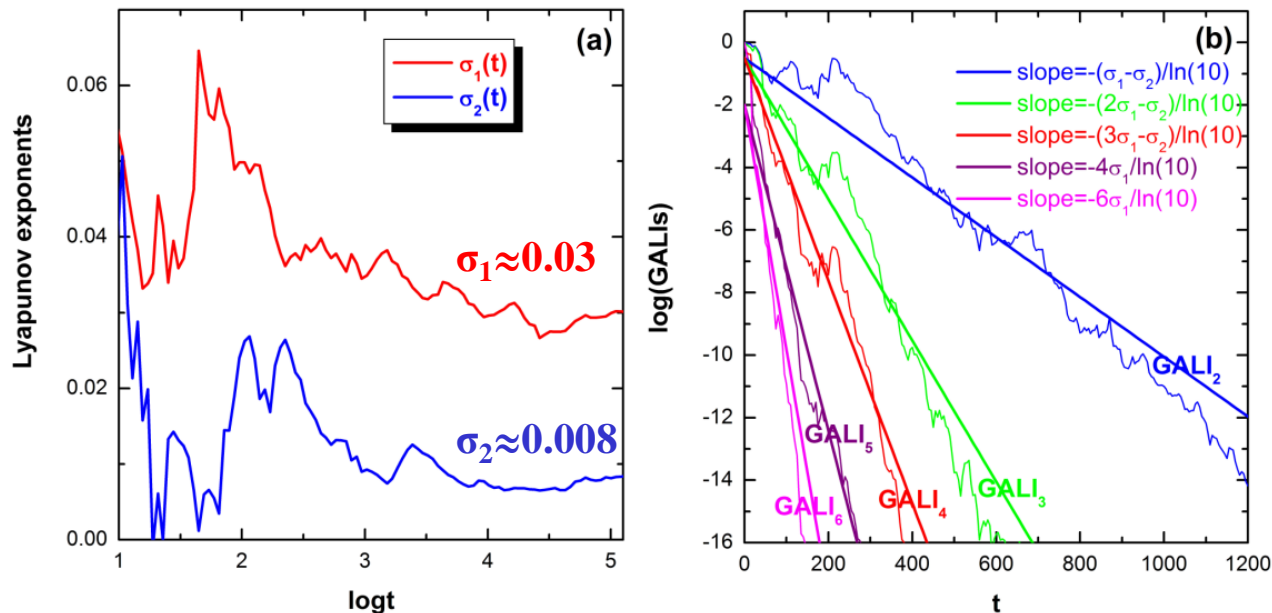


Behavior of GALI_k for chaotic motion

3D system:

$$H_3 = \sum_{i=1}^3 \frac{\omega_i}{2} (q_i^2 + p_i^2) + q_1^2 q_2 + q_1^2 q_3$$

with $\omega_1=1$, $\omega_2=\sqrt{2}$, $\omega_3=\sqrt{3}$, $H_3=0.09$.



Behavior of GALI_k for regular motion

If the motion occurs on an **s-dimensional torus** with $s \leq N$ then the behavior of GALI_k is given by (Ch.S., Bountis, Antonopoulos, 2008, Eur. Phys. J. Sp. Top.):

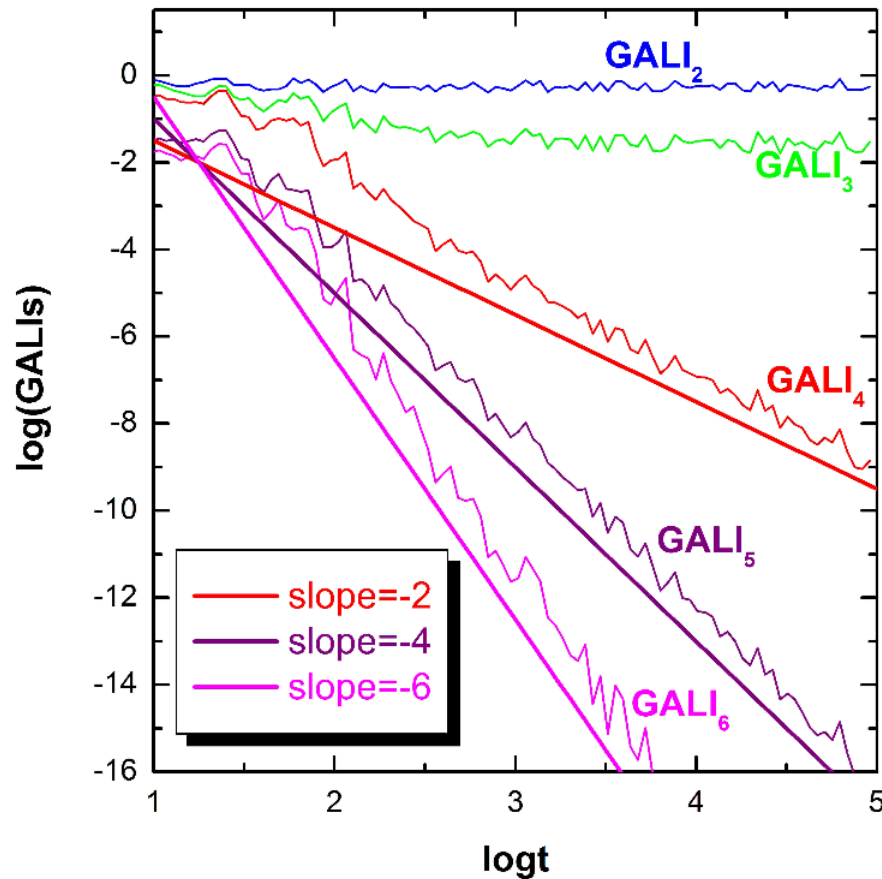
$$\text{GALI}_k(t) \propto \begin{cases} \text{constant} & \text{if } 2 \leq k \leq s \\ \frac{1}{t^{k-s}} & \text{if } s < k \leq 2N - s \\ \frac{1}{t^{2(k-N)}} & \text{if } 2N - s < k \leq 2N \end{cases}$$

while in the **common case with $s=N$** we have :

$$\text{GALI}_k(t) \propto \begin{cases} \text{constant} & \text{if } 2 \leq k \leq N \\ \frac{1}{t^{2(k-N)}} & \text{if } N < k \leq 2N \end{cases}$$

Behavior of GALI_k for regular motion

3D Hamiltonian



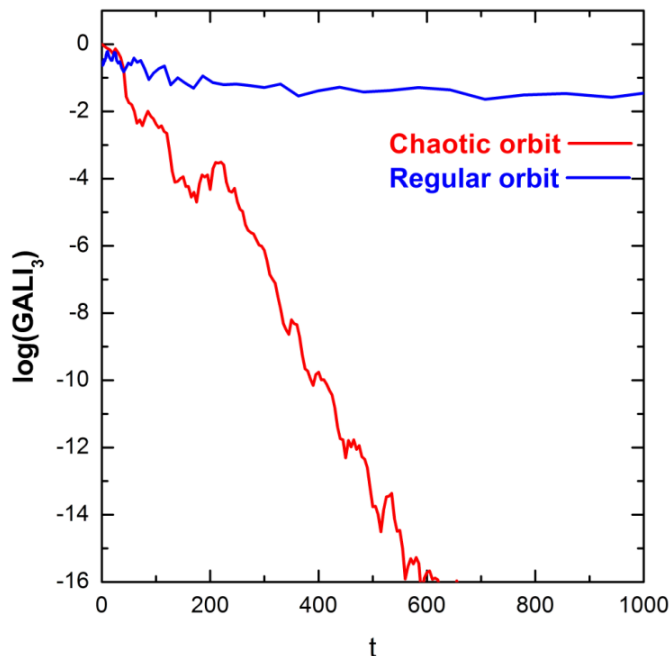
Global dynamics

- GALI_2 (practically equivalent to the use of SALI)

- GALI_N

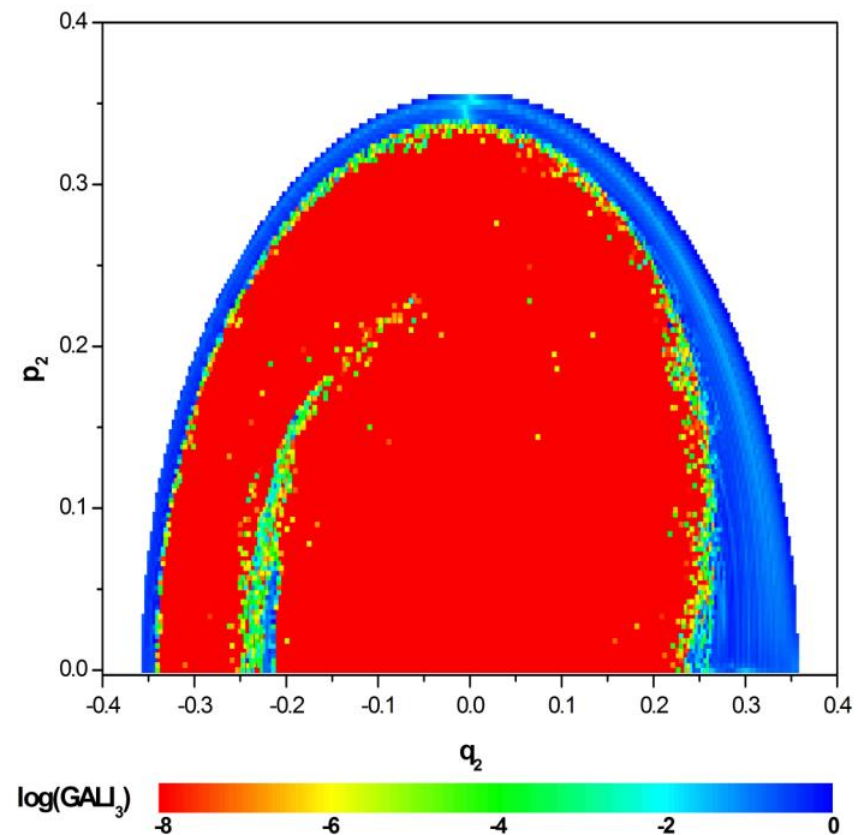
Chaotic motion: $\text{GALI}_N \rightarrow 0$
(exponential decay)

Regular motion:
 $\text{GALI}_N \rightarrow \text{constant} \neq 0$



3D Hamiltonian

Subspace $q_3=p_3=0$, $p_2 \geq 0$ for $t=1000$.



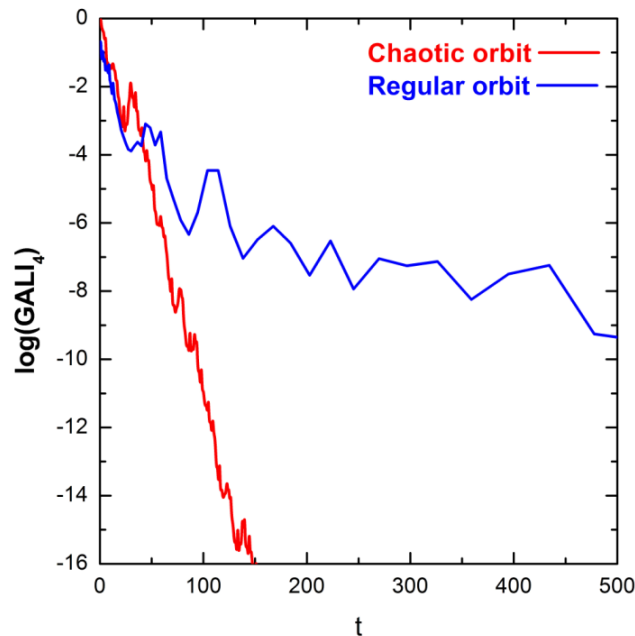
Global dynamics

GALI_k with $k > N$

The index tends to zero both for regular and chaotic orbits but with completely different time rates:

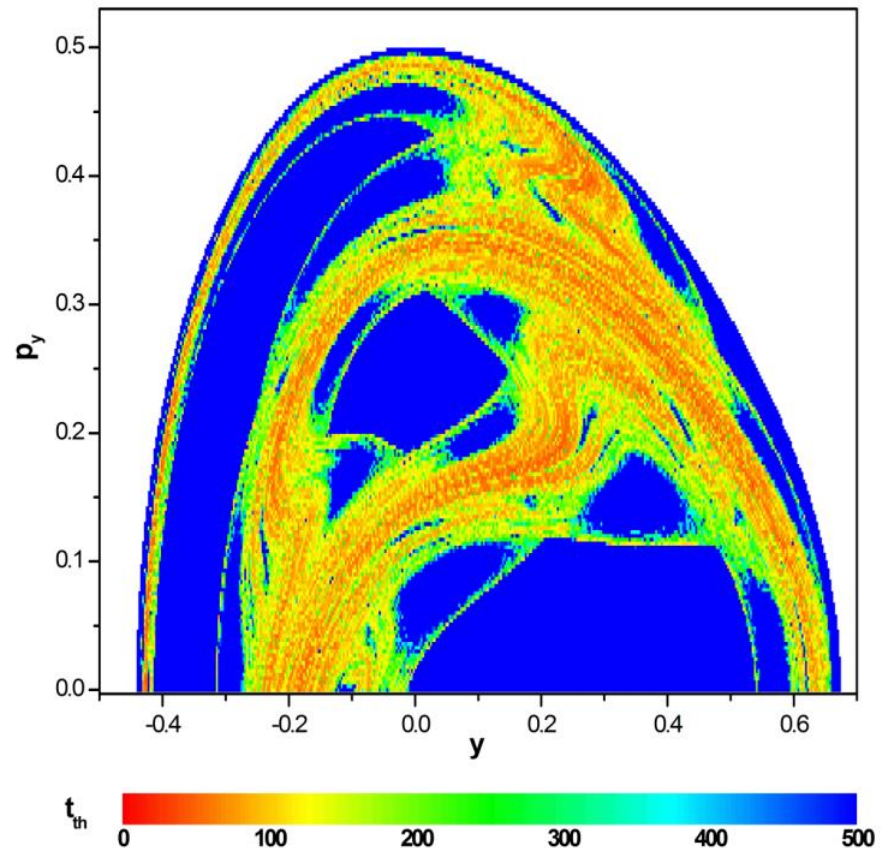
Chaotic motion: exponential decay

Regular motion: power law



2D Hamiltonian (Hénon-Heiles)

Time needed for $\text{GALI}_4 < 10^{-12}$



Behavior of $GALI_k$

Chaotic motion:

$GALI_k \rightarrow 0$ exponential decay

$$GALI_k(t) \propto e^{-[(\sigma_1 - \sigma_2) + (\sigma_1 - \sigma_3) + \dots + (\sigma_1 - \sigma_k)]t}$$

Regular motion:

$GALI_k \rightarrow \text{constant} \neq 0$ or $GALI_k \rightarrow 0$ power law decay

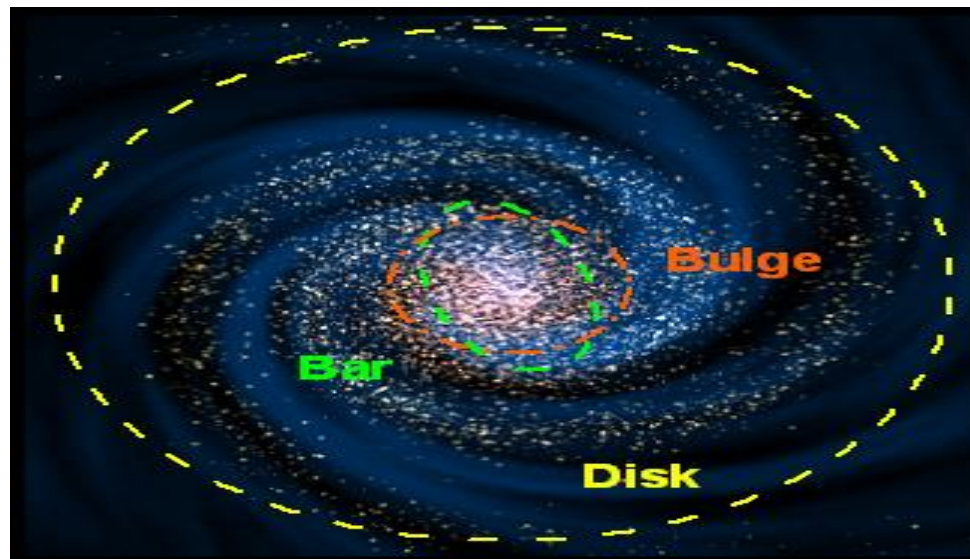
$$GALI_k(t) \propto \begin{cases} \text{constant} & \text{if } 2 \leq k \leq s \\ \frac{1}{t^{k-s}} & \text{if } s < k \leq 2N-s \\ \frac{1}{t^{2(k-N)}} & \text{if } 2N-s < k \leq 2N \end{cases}$$

Barred galaxies

NGC 1433



NGC 2217



Barred galaxy model

The 3D bar rotates around its short z -axis (x : long axis and y : intermediate). The Hamiltonian that describes the motion for this model is:

$$H = \frac{1}{2}(p_x^2 + p_y^2 + p_z^2) + V(x, y, z) - \Omega_b(xp_y - yp_x) \equiv \text{Energy}$$

This model consists of the superposition of potentials describing an **axisymmetric** part and a **bar** component of the galaxy (**Manos, Bountis, Ch.S., 2013, J. Phys. A**).

a) Axisymmetric component:

i) **Plummer sphere:**

$$V_{\text{sphere}}(x, y, z) = -\frac{GM_s}{\sqrt{x^2 + y^2 + z^2 + \epsilon_s^2}}$$

ii) **Miyamoto–Nagai disc:**

$$V_{\text{disc}}(x, y, z) = -\frac{GM_D}{\sqrt{x^2 + y^2 + (A + \sqrt{B^2 + z^2})^2}}$$

b) Bar component: $V_{\text{bar}}(x, y, z) = -\pi Gabc \frac{\rho_c}{n+1} \int_{\lambda}^{\infty} \frac{du}{\Delta(u)} (1 - m^2(u))^{n+1},$

(Ferrers bar)

$$\rho_c = \frac{105}{32\pi} \frac{GM_B}{abc}$$

$$\text{where } m^2(u) = \frac{x^2}{a^2 + u} + \frac{y^2}{b^2 + u} + \frac{z^2}{c^2 + u}, \Delta^2(u) = (a^2 + u)(b^2 + u)(c^2 + u),$$

n : positive integer ($n = 2$ for our model), λ : the unique positive solution of $m^2(\lambda) = 1$

Its density is:

$$\rho = \begin{cases} \rho_c (1 - m^2)^n, & \text{for } m \leq 1 \\ 0, & \text{for } m > 1 \end{cases}, \text{ where } m^2 = \frac{x^2}{a^2} + \frac{y^2}{b^2} + \frac{z^2}{c^2}, a > b > c \text{ and } n = 2.$$

Time-dependent barred galaxy model

The 3D bar rotates around its short z -axis (x : long axis and y : intermediate). The Hamiltonian that describes the motion for this model is:

$$H = \frac{1}{2}(p_x^2 + p_y^2 + p_z^2) + V(x, y, z, t) - \Omega_b(xp_y - yp_x) \equiv \text{Energy}$$

This model consists of the superposition of potentials describing an **axisymmetric** part and a **bar** component of the galaxy (Manos, Bountis, Ch.S., 2013, J. Phys. A).

a) Axisymmetric component:

$$M_S + M_B(t) + M_D(t) = 1, \text{ with } M_B(t) = M_B(0) + \alpha t$$

i) **Plummer sphere:**

$$V_{\text{sphere}}(x, y, z) = -\frac{GM_S}{\sqrt{x^2 + y^2 + z^2 + \epsilon_s^2}}$$

ii) **Miyamoto–Nagai disc:**

$$V_{\text{disc}}(x, y, z) = -\frac{GM_D(t)}{\sqrt{x^2 + y^2 + (A + \sqrt{B^2 + z^2})^2}}$$

b) Bar component: $V_{\text{bar}}(x, y, z) = -\pi Gabc \frac{\rho_c}{n+1} \int_{\lambda}^{\infty} \frac{du}{\Delta(u)} (1 - m^2(u))^{n+1},$

(Ferrers bar)

$$\rho_c = \frac{105}{32\pi} \frac{GM_B(t)}{abc}$$

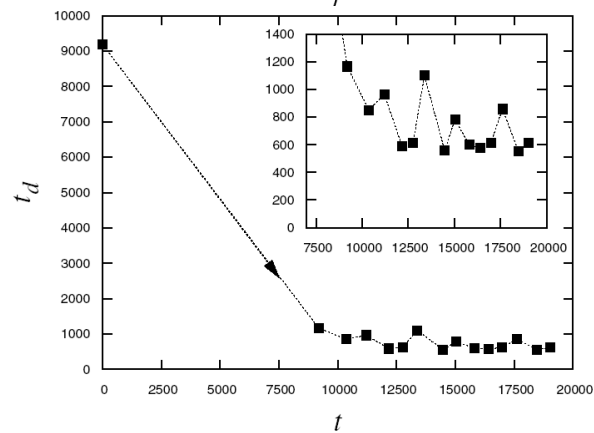
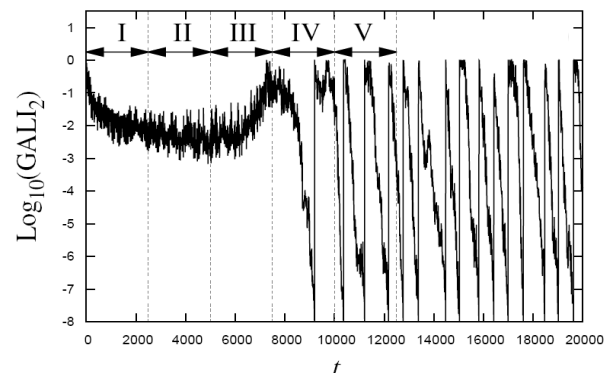
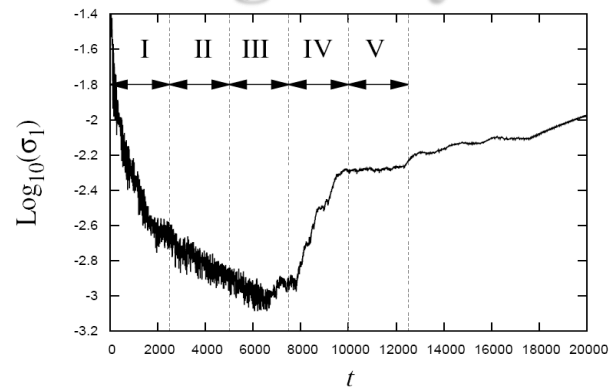
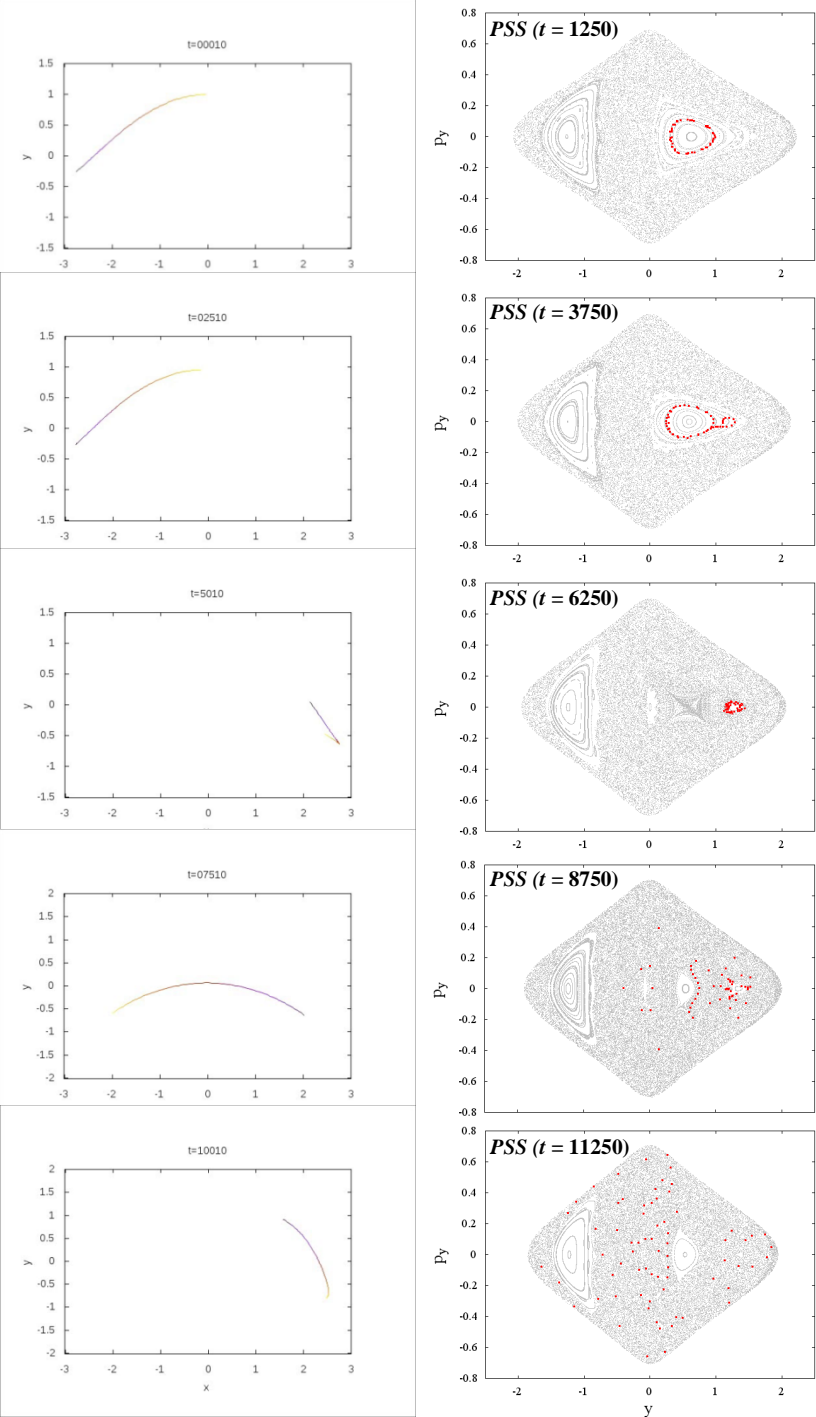
$$\text{where } m^2(u) = \frac{x^2}{a^2 + u} + \frac{y^2}{b^2 + u} + \frac{z^2}{c^2 + u}, \Delta^2(u) = (a^2 + u)(b^2 + u)(c^2 + u),$$

n : positive integer ($n = 2$ for our model), λ : the unique positive solution of $m^2(\lambda) = 1$

Its density is:

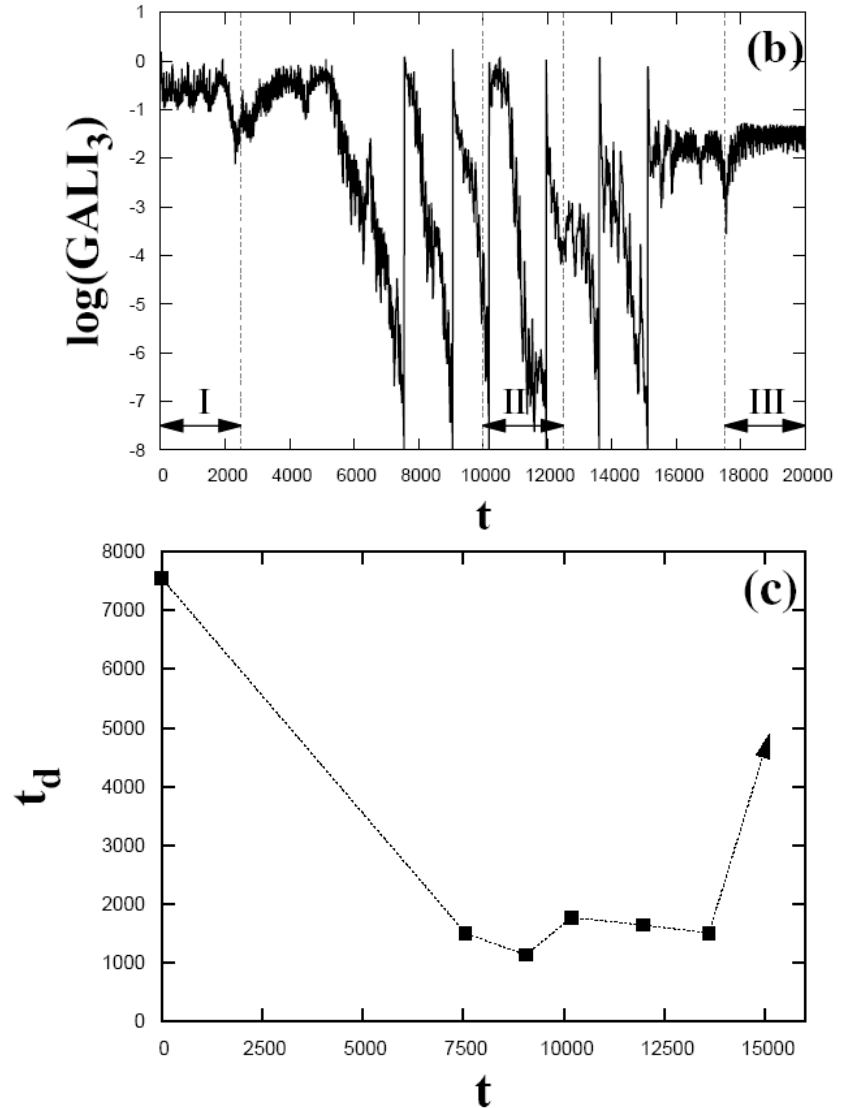
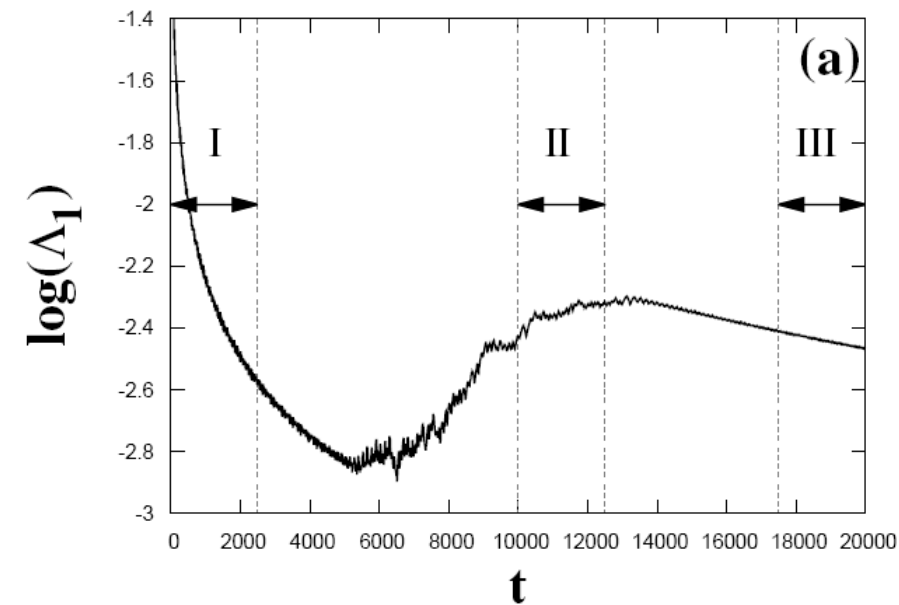
$$\rho = \begin{cases} \rho_c (1 - m^2)^n, & \text{for } m \leq 1 \\ 0, & \text{for } m > 1 \end{cases}, \text{ where } m^2 = \frac{x^2}{a^2} + \frac{y^2}{b^2} + \frac{z^2}{c^2}, a > b > c \text{ and } n = 2.$$

Time-dependent 2D barred galaxy model



Time-dependent 3D barred galaxy model

Interplay between chaotic and regular motion



Symmary

- Generalizing the SALI method we define the Generalized ALignment Index of order k ($GALI_k$) as the volume of the generalized parallelepiped, whose edges are k unit deviation vectors.
- Behaviour of $GALI_k$:
 - ✓ Chaotic motion: it tends exponentially to zero with exponents that involve the values of several Lyapunov exponents.
 - ✓ Regular motion: it fluctuates around non-zero values for $2 \leq k \leq s$ and goes to zero for $s < k \leq 2N$ following power-laws, with s being the dimensionality of the torus.
- $GALI_k$ indices :
 - ✓ can distinguish rapidly and with certainty between regular and chaotic motion.
 - ✓ can be used to characterize individual orbits as well as "chart" chaotic and regular domains in phase space.
 - ✓ are perfectly suited for studying the global dynamics of multidimentonal systems , as well as of time-dependent models.

References

- **SALI**

- ✓ Ch.S. (2001) J. Phys. A, 34, 10029
- ✓ Ch.S., Antonopoulos Ch., Bountis T. C. & Vrahatis M. N. (2003) Prog. Theor. Phys. Supp., 150, 439
- ✓ Ch.S., Antonopoulos Ch., Bountis T. C. & Vrahatis M. N. (2004) J. Phys. A, 37, 6269
- ✓ Bountis T. & Ch.S. (2006) Nucl. Inst Meth. Phys Res. A, 561, 173
- ✓ Boreaux J., Carletti T., Ch.S. & Vittot M. (2012) Com. Nonlin. Sci. Num. Sim., 17, 1725
- ✓ Boreaux J., Carletti T., Ch.S., Papaphilippou Y. & Vittot M. (2012) Int. J. Bif. Chaos, 22, 1250219

- **GALI**

- ✓ Ch.S., Bountis T. C. & Antonopoulos Ch. (2007) Physica D, 231, 30-54
- ✓ Ch.S., Bountis T. C. & Antonopoulos Ch. (2008) Eur. Phys. J. Sp. Top., 165, 5-14
- ✓ Gerlach E., Eggl S. & Ch.S. (2012) Int. J. Bif. Chaos, 22, 1250216
- ✓ Manos T., Ch.S. & Antonopoulos Ch. (2012) Int. J. Bif. Chaos, 22, 1250218
- ✓ Manos T., Bountis T. & Ch.S. (2013) J. Phys. A, 46, 254017

- **Reviews on SALI and GALI**

- ✓ Bountis T.C. & Ch.S. (2012) ‘Complex Hamiltonian Dynamics’, Chapter 5, Springer Series in Synergetics
- ✓ Ch.S. & Manos T. (2016) Lect. Notes Phys., 915, 129-181

A ...shameless promotion

Contents

Lecture Notes in Physics 915

Charalampos (Haris) Skokos
Georg A. Gottwald
Jacques Laskar *Editors*

Chaos Detection and Predictability

 Springer

1. **Parlitz:** Estimating Lyapunov Exponents from Time Series
2. **Lega, Guzzo, Froeschlé:** Theory and Applications of the Fast Lyapunov Indicator (FLI) Method
3. **Barrio:** Theory and Applications of the Orthogonal Fast Lyapunov Indicator (OFLI and OFLI2) Methods
4. **Cincotta, Giordano:** Theory and Applications of the Mean Exponential Growth Factor of Nearby Orbits (MEGNO) Method
5. **Ch.S., Manos:** The Smaller (SALI) and the Generalized (GALI) Alignment Indices: Efficient Methods of Chaos Detection
6. **Sándor, Maffione:** The Relative Lyapunov Indicators: Theory and Application to Dynamical Astronomy
7. **Gottwald, Melbourne:** The 0-1 Test for Chaos: A Review
8. **Siebert, Kantz:** Prediction of Complex Dynamics: Who Cares About Chaos?